BLACK SWANS AND SAFE HAVENS: THE ROLE OF GOLD IN GLOBALLY INTEGRATED EMERGING MARKETS

STELIOS BEKIROS[a,b], SABRI BOUBAKER[c,d], DUC K. NGUYEN[b,*], GAZI S. UDDIN[e]

[a] *European University Institute, Florence, Italy*
[b] *IPAG Business School, Paris, France*
[c] *Champagne School of Management (Groupe ESC Troyes), Troyes, France*
[d] *IRG, Université Paris-Est, Créteil, France*
[e] *Linköping University, Linköping, Sweden*

ABSTRACT

Previous studies have confirmed that Gold still acts as both a hedge and a safe haven for equity markets over recent years, and particularly during crises periods. Our work extends the recent literature on hedging and the diversification role of Gold by analyzing its interaction vis-à-vis the stock markets of the heterogeneous BRICS economies. Whilst they exhibit a high growth rate, these economies still experience a pronounced vulnerability to external shocks particularly to commodities. Via a multi-scale wavelet approach and a time-varying copula methodology, we reveal a strong time-varying asymmetric dependence structure between Gold and each of the BRICS. The multi-resolution analysis uncovers the time-scale co-evolvement patterns between the two markets, with profound regions of concentrated extreme variations. We indicate the potential implications of risk diversification and portfolio hedging strategies amongst the investigated markets.

JEL Codes: G1; C14; C32; C51
Keywords: gold; equity markets; copulas; time-scale analysis

[*] *Corresponding author***:** IPAG Business School, 184 Boulevard Saint-Germain, 75006 Paris, France. Phone: +33 01 53 63 36 02; Fax: +33 01 45 44 40 46
Email addresses: S. Bekiros (stelios.bekiros@eui.eu), S. Boubaker (sabri.boubaker@get-mail.fr), D.K. Nguyen (duc.nguyen@ipag.fr), G.S. Uddin (gazi.salah.uddin@liu.se)

1. INTRODUCTION

Brazil, Russia, India, China and South Africa (BRICS) represent the leading emerging economies in the world. After the global financial crisis 2008-2009, gold emerged as an attractive asset class with low perceived risk in an environment of systematic instability, continued low demand and deflationary pressures. The volume of gold traded in 2014 as reported by London Bullion Market Association amounted approximately to 157000 tones with a value of $5.9 trillion. In March 2013, BRICS countries signed an agreement for the creation of New Development Bank (NDB or also referred to as the BRICS Development Bank) based in Shanghai, which came into force in July 2015. The NDB aims to "*mobilize resources for infrastructure and sustainable development projects in BRICS and other emerging market economies and developing countries to complement the existing efforts of multilateral and regional financial institutions for global growth and development*".[1] For this purpose, it will be endowed with an enormous currency exchange reserve of US$100 billion backed by gold commodities. Based on reliable economic forecasts, BRICS are anticipated to exhibit exceptionally high economic growth rates over the next 50 years. According to the IMF estimates (IMF, 2015), the share of the BRICS countries in global GDP (PPP basis) is expected to be around 33% by 2020 and exceeds that of the G7 by 2017. Negative shocks affecting the BRICS economic and financial systems could thus harm seriously the global growth and financial stability.

According to previous studies, gold still acts as both a hedge and a safe haven for stocks particularly during crises periods, albeit not identically for all international markets. In our work, we extend the recent literature on hedging and diversification benefits of gold by analyzing its interactions with stock markets within the heterogeneous BRICS economies. While experiencing a high growth rate, these economies still present signs of high vulnerability to external shocks and commodity dependence. Baur and McDermott (2010) and Miyazaki *et al.* (2012) have all reported gold's safe-haven status with respect to stock market movements. Moreover Baur and

[1] http://brics.itamaraty.gov.br/media2/press-releases/219-agreement-on-the-new-development-bank-fortaleza-july-15

Lucey (2010) using daily data from 1995 to 2005 found that gold is on average a fair hedge against stocks and a safe haven in extreme stock market conditions. Hammoudeh *et al.* (2011) have highlighted the importance of other precious metals besides gold in risk management whilst Conover *et al.* (2009) suggested that investors could considerably improve portfolio performance by adding a significant exposure to the equities of precious metals. Riley (2010) also showed that precious metals in general have notable advantages like high expected returns and strong negative correlations vis-à-vis other asset classes.

More recently, Baur (2013) via introducing seasonality into monthly gold prices from 1980 to 2010 showed that September and November were the only months with positive and statistically significant gold price changes specifically called the "autumn effect". Using a model of dynamic conditional correlation, Joy (2011) investigated the practical investment question of whether gold could act as a hedge against the US dollar. During the past 23 years, he found that it has behaved quite consistently. Furthermore through the application of copulas, Reboredo (2013) assessed the role of gold as a safe haven against the USD and demonstrated that the significantly positive unconditional dependence between gold and dollar depreciation is consistent with the fact that gold can act as hedge against USD fluctuations. He also founds that there exists a symmetric tail dependence between gold and USD rates, indicating that gold could be considered effective even against extreme upside or downward USD movements.

In this work, we extend this recent literature on the diversification advantages of gold by analyzing its interactions and dependence structure against the BRICS stock markets. Firstly, we improve the common understanding of gold-stock market linkages by looking not only at the dynamic series interdependence on an aggregate level, but also at their scale-by-scale interaction utilizing a time-frequency framework. Relying on continuous and wavelet transforms as well as on time-varying copula modeling, we show evidence of a volatile dependence structure between gold and each one of the BRICS markets. Secondly, a "phase-cycle" coherence analysis between the BRICS and the gold market reveals that gold consistently and significantly leads equity markets during the recent financial crisis. However, strong heterogeneity is observed between gold-equity pairs after the implementation of a frequency-domain causality analysis. Thirdly, in an attempt to model the second moment behavior of all markets, we illustrate that the implementation of a GJR-GARCH filter provides with statistically significant asymmetric effects, especially concerning the dependence between the stock South African and the Gold commodity market. Generally, the copula analysis showed that the lower tail dependence is larger than the upper tail one for all BRICS, a fact that indicates a stronger comovement of BRICS stock markets and gold during bear rather than in bull markets. Our results from the multi-scale analysis uncover the disaggregate time-scale convolution patterns between the two markets with often profound extreme variations. Finally we discuss the potential implications of our results on the equity portfolio risk diversification and efficient hedging strategies.

The remainder of the article is organized as follows: Section 2 describes the data and performs a preliminary analysis. Section 3 presents the novel methodology based on time-scale spectral and copula approaches, while Section 4 reports and discusses the results. Section 5 concludes.

2. DATA AND PRELIMINARY ANALYSIS

We consider a set of MSCI indices for the BRICS to avoid the domestic inflation problem and the 3-month futures prices for gold, the latter of which efficiently incorporate expectations about forecasted gold demand. We use daily data as they are better to measure extreme dependence, spanning the period January 2000 to July 2014. Our dataset includes the global financial crisis of 2007-2009 wherein as well as onwards, gold prices exhibited long swings and unstable fluctuations. Hence, we could investigate the role of the gold market vis-à-vis the BRICS economies during both in normal and crisis periods. We use logarithmic returns for all series.

Based on the descriptive statistics (Table 1) we see that India has on average a higher daily return (0.030%) compared to the rest of the BRICS, whereas gold return (0.039%) is slightly higher. The unconditional volatility is higher for Russia followed by Brazil, China, South Africa, India and gold. As all returns are negatively skewed for the gold market and the BRICS and kurtosis is greater than three we infer that all examined markets are not normally distributed, a fact that is further substantiated by the Jarque-Bera test. In addition, we compute the Ljung-Box and the Engle (1982) test. The results of the Ljung-Box test applied for the case of a 12-order autocorrelation are significant for all series. The ARCH test for 12 lags provides with strong evidence of conditional heteroscedasticity in all return series. Stationarity and unit root tests applied on all series conclude that price variables are not stationary, while returns are stationary at all conventional significance levels. The optimum lag length is selected based on the Schwarz Information Criterion (SIC) [2]. Next, we observe that a weak positive correlation (0.09) is found between gold and China equity market followed by India (0.11), Russia (0.12), Brazil (0.15) and South Africa (0.28) respectively. Those moderately weak unconditional correlations may imply portfolio diversification benefits from investing in BRICS equity markets and the gold derivatives market. The observed instability in the BRICS markets could be rationalized by the impact of the different economic and financial crises since 2008. This result could be visually inspected in Figures 1 and 2. Furthermore, the gold prices are upward until 2012 as also displayed in the corresponding Figures, whereas from the second quarter of 2013 onwards the recent decline in gold price has probably generated a significant increase in overall demand in China and India compared to the same time period for 2014. After the Lehman Brothers collapse and the subsequent Subprime crisis, China and Russia proceeded in incorporating gold as an integral part of their newly designed monetary system in an attempt to counterbalance the consequences for the bond and stock US markets as well as compete in terms of capital inflows. Those results have been also reported by the World Gold Council (2014). Therefore, the issue of possible hedging and diversification benefits from investing in gold is fundamentally important for industrialized countries, yet only recently became of utmost importance for the BRICS economies as well.

[2] Results are available upon request.

3. METHODOLOGY

3.1 Frequency-domain causality analysis

Firstly, we investigate the nature and direction of interdependencies as well as the spillover effects between the BRICS equity markets and gold futures' market, utilizing a frequency-domain causality analysis. The standard Granger causality test ignores the possibility that the strength and direction of the detected causality (if any) can vary over different frequencies or time horizons as reported in Lemmens *et al.* (2008). To overcome this crucial issue Breitung and Candelon (2006) developed a variation of the standard causality test in the frequency domain based on the works by Granger (1969) and Geweke (1982).[3] Specifically, Breitung and Candelon (2006) would express the relationship between equity series (E_t) and gold returns (G_t) under a Vector Autoregressive (VAR) model:

$$\begin{cases} E_t = a_1 E_{t-1} + ... + a_p E_{t-p} + \beta_1 G_{t-1} + ... + \beta_p G_{t-p} + \varepsilon_{1t} \\ G_t = b_1 G_{t-1} + ... + b_q G_{t-q} + \alpha_1 E_{t-1} + ... + \alpha_p E_{t-q} + \xi_{1t} \end{cases} \quad (3)$$

In order to test the hypothesis that *gold* does not cause *equities* in the frequency interval $\vartheta \in (0, \pi)$, Geweke developed the null as $M_{y \to x}(\vartheta) = 0$, within a bivariate framework such as:

$$H_0 : R(\vartheta)\beta = 0 \quad (4)$$

where β is the vector of the coefficients and

$$R(\vartheta) = \begin{bmatrix} \cos(\vartheta)\cos(2\vartheta).....\cos(p\vartheta) \\ \sin(\vartheta)\sin(2\vartheta).......\sin(p\vartheta) \end{bmatrix} \quad (5)$$

The F-statistic under the null is approximately distributed as $F(2, T-2p)$ within $\vartheta \in (0, \pi)$. It is worth noting that the particular frequency domain causality test can also be conducted under a cointegrating framework. Breitung and Candelon (2006) suggest that in cointegrated systems the definition of causality at zero frequency is equivalent to the concept of long-run causality. In our

[3] This causality approach has been previously implemented in the analysis of monetary policy and its impact on financial markets e.g., by Assenmacher-Wesche and Gerlach (2007), Assenmacher-Wesche *et al.* (2008), Lemmens *et al.* (2008) and Gronwald (2009) among others.

study we tested for cointegration and we were not able to detect it, hence the stationary VAR of the return series is well-specified.[4] According to Breitung and Candelon (2006), the presence of causality between variables at different frequencies implies that specific frequency components of one variable can be predicted by those of the other variable.

3.2 Coherence analysis of co-movement

The commonly used Breitung and Candelon (2006) test provides causality results only at some pre-specified frequency range $[\alpha, \beta]$. The right value β represents the lowest frequency upon which the test can infer on causality. According to Bekiros and Marcellino (2013) employing multi-scale wavelet analysis provides an efficient means of overcoming the constraint of reaching a threshold in the lowest possible frequency investigated, hence probing further in the long- and short-run behavior of the variables. Bekiros and Marcellino (2013) also argue that as the Breitung and Candelon test is based on vector autoregressive modelling, it cannot reveal nonlinear interrelationships of 2nd or higher order as opposed to wavelet coherency approach utilized in this work. Via time-scale wavelet analysis we can detect time-varying links between gold and the BRICS markets under a time-frequency framework. Overall, wavelets are not restricted to a pre-specified frequency range imposed by the raw data frequency.

The flurry of interest in economic applications of multi-resolution analysis occurred in the mid-90s mostly by Ramsey and his collaborators. Ramsey, Usikov and Zaslavsky (1995) pursued a wavelet approach in detecting self-similarity in US stock prices, whilst Ramsey and Lampart (1998a, 1998b) used a wavelet-based scaling method to investigate the relationship and causality between money, income and expenditure. Their contribution was enhanced by Gençay and co-authors (e.g., Gençay *et al.,* 2001; Gençay *et al.,* 2002; Fan and Gençay, 2010) and in particular by the seminal work of Gençay *et al.* (2002) on the introduction of wavelet multiresolution analysis in finance and economics.

[4] More details on this issue as well as on the frequency causality testing of $I(1)$ variables can be found in Breitung and Candelon (2006).

In our work we focus on the continuous wavelet transform (CWT) to analyze the phase synchronization and co-movement of the gold market and the BRICS and the maximal overlap discrete wavelet transform (MODWT) to investigate the time-scale dynamic causal links. The wavelet coherence allows identifying the phase or anti-phase between oscillations of the variables signals under investigation (Aguiar-Conraria and Soares, 2014).

The CWT specification following by Rua and Nunes (2009) uses the continuous Morlet wavelet function $\psi_{\sigma}(t)$ with a frequency parameter equal to six.[5] The continuous wavelet transform $W_t^E(r)$ of a discrete sequence $x_m\left(m=1,\ldots,M-1,M\right)$ with uniform time steps δ_t is defined as the convolution of x_m with the scaled and normalized wavelet. The equation can be expressed as:

$$W_t^E(r) = \sqrt{\frac{\delta t}{r}} \sum_{t=1}^{M} x_{m'} \psi_{\sigma}\left[(m' - m)\frac{\delta t}{r}\right] \qquad (6)$$

where δ is the time step. The wavelet power is defined as $|W_t^E(r)|^2$. In our CWT sepcification, the wavelet coherence is the most suitable tool for measuring the extent of synchronization between the gold market and the BRICS economies both over time and across scales. It is defined as the ratio of the cross power spectrum of two series over the product of each series' power spectrum, thus it may be interpreted as the localized correlation between the series under consideration. Let E_t be each of the BRICS equity market and G_t the gold futures' market with wavelet power spectra $W_t^E(r)$ and $W_t^G(r)$ respectively. The cross-wavelet power spectrum is defined as $W_t^{EG}(r) = W_t^E(r) * W_t^G(r)$ whilst their coherence measure is estimated computed as in Torrence and Webster (1999):

$$\mathrm{R}_\mathrm{t}^2(\mathrm{r}) = \frac{\left|\mathrm{Q}\left(\mathrm{r}^{-1}\mathrm{W}_\mathrm{t}^{\mathrm{EG}}(\mathrm{r})\right)\right|^2}{\mathrm{Q}\left|\left(\mathrm{r}^{-1}\left|\mathrm{W}_\mathrm{t}^{\mathrm{E}}(\mathrm{r})\right|^2\right)\right|.\mathrm{Q}\left|\left(\mathrm{r}^{-1}\left|\mathrm{W}_\mathrm{t}^{\mathrm{G}}(\mathrm{r})\right|^2\right)\right|} \qquad (7)$$

[5] In a robustness analysis we utilized various different functions, yet the results are not significantly modified in the empirical application.

where Q refers to a smoothing operator (Rua and Nunes, 2009). The numerator is the absolute squared value of the smoothed cross-wavelet spectrum, while the denominator is the product of the smoothed wavelet power spectra (Torrence and Webster, 1999; Rua and Nunes, 2009). The value of the wavelet squared coherence $R_t^2(r)$ is bounded between 0 and 1. However unlike the standard correlation coefficient, the wavelet coherence measure only takes positive values i.e., evaluating the strength of the co-movement/relationship from extremely weak to very strong. As in Torrence and Compo (1998), we use Monte Carlo simulation methods are used to generate the statistical significance of the coherence measure.

3.3 Multivariate dependence structure: Copulas

In studying the dynamic inter-linkages of our variables we depend upon multivariate copula analysis. Modeling dependence using copula functions is appealing as they offer flexibility in modeling separately the marginals, are invariant to monotonic transformations of the variables as well as they provide information on both average dependence and tail dependence.

Let $R_{s,t}$ and $R_{g,t}$ be random variables denoting BRICS's stock and gold future returns (s→BRICS and g→gold) respectively, at time t. Moreover, let their conditional continuous cumulative distribution functions (CDFs) be $F_s\ (R_{s,t|}\psi_{t-1})$ and $F_g\ (R_{g,t|}\psi_{t-1})$ respectively, where ψ_{t-1} denotes all past return information for the corresponding assets. Sklar's theorem (Patton, 2006) states that the conditional joint distribution function H for $R_{s,t}$ and $R_{g,t}$ has a unique copula representation C, such that:

$$H\big(R_{s,t}, R_{g,t}|y_{t-1}\big) = \mathrm{C}\big((F_{s,t}(R_{s,t}|y_{t-1}), F_{g,t}(R_{g,t}|y_{t-1})\big) \qquad (8)$$

Assuming all CDFs are differentiable, the joint density can be obtained as:

$$h\big(R_{s,t}, R_{g,t}|y_{t-1}\big) = \frac{dH\big(R_{s,t}, R_{g,t}|y_{t-1}\big)}{dR_{s,t}, dR_{g,t}}$$

$$= \mathrm{c}\big((F_{s,t}(R_{s,t}|y_{t-1}), F_{g,t}(R_{g,t}|y_{t-1})\big)|y_{t-1}) \ \mathbf{x}\ f_{s,t}(R_{s,t}|y_{t-1}) \ \mathbf{x}\ f_{g,t}(R_{g,t}|y_{t-1})) \qquad (9)$$

where $c(u_t, v_t) = d^2C(u_t, v_t|\psi_{t-1})/du_t dv_t$ with $u_t = F_s(R_{s,t|}\psi_{t-1})$ and $v_t = F_g(R_{g,t|}\psi_{t-1})$ representing the conditional copula density. Thus, the conditional bivariate density function $h(R_{s,t}, R_{g,t}|y_{t-1})$ is represented by the product of the copula density and the two conditional marginal densities $f_{s,t}$ $(R_{s,t|}\psi_{t-1})$ and $f_{g,t}$ $(R_{g,t|}\psi_{t-1})$. Accordingly, the log-likelihood function can be written as:

$$log\left[h\left(R_{s,t}, R_{g,t}|y_{t-1}\right)\right] = \log\left[c(F_{s,t}(R_{s,t}|y_{t-1})\right] + \log\left[f_{s,t}(R_{s,t}|y_{t-1})\right] + \log\left[f_{g,t}(R_{g,t}|y_{t-1})\right] \quad (10)$$

The parameters for the copula density and the marginal functions can be obtained by maximizing Eq. (10) using the two-step estimation procedure proposed by Joe (1997) called "*Inference for Margins*" approach (IFM). This consists of first obtaining the marginal density parameters for both marginals via maximum likelihood and then using these estimates to obtain the copula parameters (q_g) by solving the following expression:

$$\widehat{q_g} = argmax \sum_{t=1}^{T} \ln c(\widehat{u_t}, \widehat{v}_t\,; q_g) \qquad (11)$$

where $\widehat{u_t} = F_{s,t}(R_{s,t}|y_{t-1}; \widehat{q_c})$, $\widehat{v_t} = F_{g,t}(R_{g,t}|y_{t-1}; \widehat{q_g})$ and $\widehat{q_g}$, $\widehat{q_c}$ are the estimates of the marginal density parameters. The lower (left) and upper (right) tail dependence can be written in terms of the copula functions respectively as:

$$\lambda_L(v) = \lim_{v \to o} P\left[X \le F_g^{-1}(v) | Y \le F_s^{-1}(v)\right] = \lim_{v \to o} \frac{C(v,v)}{v} \qquad (12)$$

$$\lambda_U(v) = \lim_{v \to 1} P\left[X \ge F_g^{-1}(v) | Y \ge F_s^{-1}(v)\right] = \lim_{v \to 1} \frac{1-2v+C(v,v)}{1-v} \qquad (13)$$

where $\lambda_L(v), \lambda_U(v) \in [0.1]$. The two variables exhibit lower (upper) tail dependence if $\lambda_L > 0$ ($\lambda_U > 0$), indicating a non-zero probability of observing an extremely small (large) value for one series together with an extremely small (large) value for the other series.

To model the dependence structure, we consider various types of copula functions with symmetric and asymmetric tail behavior and time-varying dependence. The bivariate normal and student-*t* copula is defined as follows:

$$C^{Normal}(u_t, v_t\,;\, \rho) = \Phi(\Phi^{-1}(u_t), \Phi^{-1}(v_t)) \quad (14)$$

$$C^{Student-t}(u_t, v_t\,;\, r, v) = T_v(t_v^{-1}(u_t), t_v^{-1}(v_t)) \quad (15)$$

where Φ is the bivariate standard normal CDF with correlation ρ (-1< ρ<1), $\Phi^{-1}(u_t)$ and $\Phi^{-1}(v_t)$ are the standard normal quantile functions and T is the bivariate Student-t CDF with degree-of-freedom parameter and correlation ρ (-1< ρ <1). Let $t_v^{-1}(u_t)$, and $t_v^{-1}(v_t)$ be the quantile functions of the univariate Student-*t* distributions. Both copulas display symmetric dependence, even though the Gaussian has zero tail dependence and the Student-*t* displays tail dependence given by $\lambda_L = \lambda_U = 2t_{v+1}(-\sqrt{v+1}\sqrt{1-\rho}/\sqrt{1+\rho > 0}$. Next, we consider two other copulas with symmetric tail dependence, namely the Plackett and the Frank copulas, specified respectively as:

$$C^{Plackett}(u_t, v_t\ ;\ \pi) =$$

$$\frac{1}{2(\pi-1)}(1+(\pi-1)((u_t)+(v_t))) - \sqrt{(1+(\pi-1)((u_t)+(v_t)))^2 - 4\pi(4\pi-1)}u_t v_t \quad (16)$$

$$C^{Frank}(u_t, v_t\ ;\ \lambda) = \frac{-1}{\lambda}\log\left[\frac{(1-e^{-\lambda})-(1-e^{-\lambda\mu_t})(1-e^{-\lambda v_t})}{(1-e^{-\lambda})}\right] \quad (17)$$

where $\pi \in [0,\infty]\backslash\{1\}$ and $\lambda \in [-\infty,\infty]\backslash\{0\}$. Both copulas display tail independence.

Given that dependence may change under different market circumstances (in booms or bursts) we consider copula functions with asymmetric tail dependence structures as well. The Gumbel copula reflects upper tail dependence, whereas its rotation reflects lower tail dependence as follows:

$$C^{Gumbel}(u_t, v_t\ ;\ \delta) = \exp(-((-\log u_t)^{\delta} + (-\log v_t)^{\delta})^{1/\delta}) \quad (18)$$

$$C^{Rotated\_Gumbel}(u_t, v_t\ ;\ \delta) = u_t + v_t - 1 + C^{Gumbel}(1-u_t, 1-v_t\ ;\ \delta) \quad (19)$$

with $\delta \in [1,\infty]$. The upper and lower tail dependence structure of the Gumbel copula is given by $= 2 - 2^{1/\delta}$ and $\lambda_L = 0$ respectively, while the opposite holds for the rotated Gumbel. We also employ the symmetrized Joe-Clayton (SJC) copula as it simultaneously considers lower and upper tail dependence, determining the presence or absence of asymmetry:

$$C^{SJC}(u_t, v_t\ ;\ \lambda_U^{SJC}, \lambda_L^{SJC}) = 0.5(C^{JC}(u_t, v_t\ ;\ \lambda_U^{JC}, \lambda_L^{JC}) + C^{SJC}(1-u_t, 1-v_t\ ;\ \lambda_U^{SJC}, \lambda_L^{SJC}) + u_t + v_t - 1) \quad (20)$$

where, $C^{JC}(u_t, v_t\ ;\ \lambda_U^{JC}, \lambda_L^{JC}) = 1 - (1 - \{[1 - (1 - u_t)^k]^{-\gamma} + [1 - (1 - v_t)^k]^{-\gamma}\}^{-1/\gamma})^{1/k}$ and $k = 1/log_2(2 - \lambda_U^{JC})$ and $\gamma = -1/log_2(\lambda_L^{JC})$. Moreover, $\lambda_U^{SJC}(v) \in [0,1]$ and $\lambda_L^{SJC}(v) \in [0,1]$. For this copula function, the tail dependence coefficients are themselves the parameters of the copula. In case $\lambda_U^{SJC} = \lambda_L^{SJC}$ then the market structure is symmetric, otherwise it is asymmetric.

We finally account for time-varying dependence structure by allowing the copula parameters to be time-varying with dynamics described in an evolution equation. For the Gaussian and Student-*t* copulas, we describe the dynamics of the linear dependence parameter as evolving over time according to the dynamic model proposed by Patton (2006):

$$\rho_t = \Omega(\Psi_0 + \Psi_0 \rho_{t-1} + \Psi_2 \frac{1}{10} \sum_{j=1}^{10} \Phi^{-1}(u_{t-j}) . \Phi^{-1}(v_{t-j}) \quad (21)$$

where Ω denotes the logistic transformation $\Omega(x) = (1 - e^{-x})(1 - e^{-x})^{-1}(x)$ used to keep ρ_t within (-1,1). For the Student-*t* copula, $\Phi^{-1}(x)$is substituted as $t^{-1}_v(x)$. For the conditional Gumbel copula and its rotation, the evolution of δ specified follows an ARMA(1,10) process given by:

$$d_t = (\Psi_0 + \Psi_0 d_{t-1} + \Psi_2 \frac{1}{10} \sum_{j=1}^{10} |u_{t-j} - v_{t-j}| \quad (22)$$

For the SJC copula, the evolution of upper and lower tail dependence is given by an AR-MA(1,10) process as:

$$\tau_{U,t}^{SJC} = \Omega\left[\Psi_0^U + \Psi_1^U \tau_{U,t-1}^{SJC} + \Psi_2^U \frac{1}{10} \sum_{j=1}^{10} |u_{t-j} - v_{t-j}|\right] \quad (23)$$

$$\tau_{L,t}^{SJC} = \Omega\left[\Psi_0^L + \Psi_1^L \tau_{U,t-1}^{SJC} + \Psi_2^L \frac{1}{10} \sum_{j=1}^{10} |u_{t-j} - v_{t-j}|\right] \quad (24)$$

3.4 Incorporating second-moment spillover effects

Finally, we study the parameter estimates of the marginal distributions for the BRICS equity markets and gold incorporating spillover effects via GARCH-class models. As the choice of the most suitable GARCH-type model specification appears to be challenging task, we consider standard competing models: standard GARCH, EGARCH, GJR-GARCH and FIGARCH. Based on the *Log (L)* and *SIC* criteria, we select the GJR-GARCH(1,1) as the best second-moment model for both markets. The GJR-GARCH specification is proposed by Glosten, Jagannathan and Runkle (1993) and includes a leverage term to model asymmetric volatility. In the GJR-GARCH model, large negative changes are more likely to be followed by large negative changes than positive changes. The GJR model is only a simple extension of the GARCH model, with an additional term added to capture possible asymmetries:

$$\sigma_t^2 = \omega + \alpha\varepsilon_{t-1}^2 + \beta\sigma_{t-1}^2 + \gamma\varepsilon_{t-1}^2 I_{t-1} \qquad (25)$$

where $I_{t-1}=1$ if $\varepsilon_{t-1}<0$ and otherwise $I_{t-1}=0$. According to Glosten *et al.* (1993) the positivity and stationarity of the volatility process is guaranteed whenever the parameters satisfy the constraints $\omega>0$, α, β, $\gamma\geq 0$, and $\gamma+(\alpha+\beta)/2 <1$. Lastly, we assume that the error term follows the Skewed-*t* distribution to account for clustering tails.

4. EMPIRICAL RESULTS

We explore the interrelationships between the BRICS' equity markets and the 3-month futures' Gold market at various investment horizons which directly correspond to different wavelet components. The CWT can be particularly important in investigating the scale-dependent (a)synchronization between those markets. As opposed to simple unconditional or conditional linear correlation, the wavelet coherence measure detects time-varying linear and nonlinear phase-dependent linkages via the cross-wavelet power spectrum. The application of the proposed methodology will reveal the heterogeneity of market participants and their investment horizons in both markets. Practically, short-term investors are interested in interim price fluctuations whilst long-term agents trade the long-run price movements.

Firstly, we present in Figure 3 the contour graphs of the cross-wavelet coherency for the return series between gold market and the BRICS. The thick black contour lines illustrate the 95% confidence intervals estimated from Monte Carlo simulations using phase-randomized surrogate series. The vertical axis shows the frequency (scale) and the horizontal axis, the time in days. The color presentation ranges from blue used for low coherency, to red indicating high phase co-movement. Innovatively, the coherency measure incorporates linear and nonlinear interdependencies including 2nd or higher order effects, beyond simple linear correlation relationships. In particular, the *X*-axis represents the time period explored, divided in 500, 1000, 1500, 2000, 2500, 3000 to 3500 days. The corresponding dates are 2001$M_{12}D_{03}$, 2003$M_{11}D_{03}$, 2005$M_{10}D_{03}$, 2007$M_{09}D_{03}$, 2009$M_{08}D_{03}$, 2011$M_{07}D_{04}$, and 2013$M_{06}D_{03}$ respectively, while the exact starting and ending dates are 2000$M_{01}D_{04}$ and 2014$M_{07}D_{31}$. The downward pointing "*cone of influence*" indicates the region affected by the so-called "*edge effects*", shown with a lighter shade black line. The track (direction) of the arrows provides the signal lag/lead phase relation between both the gold and equity markets. Arrows pointing to the right signify phase-synchronized series, whilst those pointing to the left indicate out-of-phase variables. Moreover, arrows pointing to the right–down or left-up indicate that gold leads the BRICS, whereas the right–up or left-down arrows reveal the reverse linkage. The in-phase regions signify a cyclical interaction between the variables while the out-of-phase (or anti-phase) behavior demonstrates an anti-cyclical effect. The contour plots derived by a three-dimensional analysis enable to detect areas of varying co-movement among the return series over time and across frequencies. Overall, the areas of stronger interdependence in the time-frequency domain imply lower benefits from international portfolio diversification. From the coherence analysis we observe that the Brazil-Gold, Russia-Gold and China-Gold market pairs, at the long-term frequency band (or short term 35-105 daily scale), demonstrate a relatively high degree of co-movement (in-phase) with the arrows pointing right, within the period 2005M10-2006M09. In the same frequency band, the South Africa-Gold pair shows a high degree of synchronization, albeit only within 2004. Next, India and Brazil equity markets display a time-varying lag-lead relationship vis-à-vis gold at different "regions" of the time-frequency state-space. During 2002M09-2003M06 and 2004M03-2004M12, namely in the (70-128) and (50-70) day-interval (long-term frequency band), the contour arrows point right-down and right-up, a fact that signifies a directional change from

Gold-leading to lagging behavior against the Brazilian market. On the other hand, for 2005M10-2006M11 and 2003M08-2004M08 and (30-105) and (40-100) day-interval the contour arrows for the India-Gold pair point right down and right-up, which indicates a directional change from leading to lagging directionality, yet now at the short term time scale. The analysis from all contours reveals a relatively high degree of co-movement between the India-Gold and China-Gold pairs concentrated at the (242-275) frequency band scales from 2003M08 to end of 2004, whereas in the similar frequency band scale, a relatively high degree of co-movement is observed between South Africa and Gold markets concentrated on the long-term frequency band which corresponds to 2001M1-2005M2. For the long-term time scale (505-610 days), Gold is leading the BRICS during 2003M11-2011M07 for Brazil and Russia, within 2007M09-2012M04 for India, in 2005M10-2011M07 for China, and during 2002M11-2011M11 for South Africa. Importantly, all through the global financial crisis (2008-2009) the gold market leads significantly the equity markets. To summarize, the wavelet phase inspection demonstrated a strong heterogeneity across scales with continuous (dynamic) directional reversals for all investigated pairs.

It is highly informative to compare the results of the cross-wavelet coherency measurement against those from the Breitung and Candelon (2006) spectral-domain test for short- and long-run causality within a wide range of frequencies in the interval $[0, \pi]$. Figure 4 illustrates the bivariate relationships amongst all investigated pairs. The frequency on the horizontal axis ϑ can be "translated" into a cycle or periodicity of T days as derived by $T = 2\pi / \vartheta$. We consider four spectral bands, i.e., very short time horizons corresponding to $\vartheta \in$ (0, 0.5), short-run horizons with $\vartheta \in$(0.5, 1.5), medium range periods of $\vartheta \in$(1.5, 2.5) and the longest time periods laying in (2.5, π). Specifically, short-term fluctuations are displayed towards the right end of the graph, long-term frequencies in the left end whilst the 5% and 10% level confidence bands are also included. The results from the spectral-domain test are in general in accordance with those from the wavelet analysis. Both bidirectional and unidirectional causalities are revealed at different frequency bands. The Brazil-Gold pair presents strong causality from Brazil equity market to gold within (0.00, 1.05) and (2.40, 2.70) frequency bands, namely both for short-run and very long-run horizons. However, the reverse dependence is observed at very short-run (0.00, 0.30), medium (1.35, 2.30) and long-term time periods corresponding to $\vartheta \in$ (2.50, 2.95). For the Russia-Gold pair, the causality runs from Russia to gold returns for $\vartheta \in$(0.00, 0.50), (0.60, 1.10), (1.35, 1.52) and (2.25, 2.70) frequency bands, whereas the reverse interrelationship is found for short- and long-run horizons. Within $\vartheta \in$(0.00, 0.90) and (2.25, 2.96) we observe causality linkages from India to gold markets whereas for $\vartheta \in$(0.00, 1.10) and (1.55, 2.40) frequency bands, the causality runs from China to gold. Interestingly, causalities emerge from the gold market to India only in the medium-term $\vartheta \in$(1.15, 1.60), as opposed to univariate links from gold to China at $\vartheta \in$(0.00, 0.60), (1.15, 1.75) and (2.40, 2.90) that correspond directly to very short-run, medium and long-run horizons. Finally, we revealed causalities from South Africa to gold markets for frequency bands laying within (0.00, 0.60), (1.40, 1.60) and (2.35, 2.70) intervals, whereas reverse linkages emerged for short-run and medium-range horizons. Nevertheless, according to Bekiros and Marcellino (2013) via the multi-scale wavelet analysis we overcome the constraint of reaching a threshold in the lowest possible frequency investigated, as well as probe further into nonlinear interrelationships of 2nd or higher order as opposed to the Breitung and Candelon test which is based on linear VAR modelling.

Next, we analyze the results from the second-moment dynamics before we proceed to the copula-based dependence structure as they will be useful for the tail modeling of the marginals. Table 2 reports the estimation results from the GJR-GARCH model for both BRICS and Gold markets. The mean equation parameters are significant in all cases except for China, while the ARCH effects are highly significant. In particular, all conditional variance terms (β) for the BRICS and gold futures' returns are significant at the 1% level. The asymmetry parameters (γ) are also significant at the 1% level in all cases as well. Interestingly, gammas (γ) affect positively the BRICS equity markets whereas the reverse is true for the gold market. Furthermore, the estimated tail parameters are strongly significant with values exceeding two, suggesting that there exists a distinctive divergence from normality. All skewness terms are negative and statistically significant, hence the Student-*t* fits all return variables well. The results of the diagnostics applied to the standardized residuals and squared residuals indicate that the GJR-GARCH model with Student-*t* error marginals is correctly specified.

Finally, Table 3 (panels A and B) exhibits the results of the tail-dependence structure. Panel A presents the estimates for the parametric copula models. Specifically, for the symmetric-class, the Student-*t* copulas perform better than the Normal, Clayton, Rotated Clayton, Plackett, Frank, Gumbel, Rotated Gumbel and Symmetrized Joe-Clayton (SJC) ones in all cases based on the AIC results. In fact, the dependence parameter for the Student-*t* copulas is quite close to the unconditional linear correlation as reported in Table 1. This outcome leads to considering the *t*-copula the best descriptor of the return dependence between BRICS equity markets and gold. The “strength” of dependence is higher for the South Africa-Gold pair, followed by the Brazil-Gold, the China-Gold, whilst the India-Gold pair appears to be the weakest. For the asymmetric tail-class copulas and in particular for the Clayton and Gumbel, the parameter estimates are significant and reflect the positive dependence between the BRICS markets and gold commodity futures market. The lower- and upper-tail dependence parameters of the Gumbel and rotated Gumbel copulas have similar values (panel A), whilst the estimated values of $\lambda LSJC$ and $\lambda USJC$ for the SJC copulas are different. Interestingly, the lower-tail parameters are higher than the upper-tail ones in all cases, thus the co-movement level of BRICS’ stock and gold markets is higher in bear markets. Lastly, according to Panel B which presents results for the time-varying copulas, the rotated Gumbel appears to provide the best description of the return dependence based on the AIC and maximum log-likelihood scores. Nevertheless, the estimated parameters for some pairs are not statistically significant, namely the time-varying copulas cannot be considered consistently superior vis-à-vis the constant ones for the investigated series. Figures 5, 6 and 7 illustrate that copula parameters change over time, e.g., for the Gumbel copula the dependence parameter ranges in (0.00-1.46) for Brazil, (0.02-1.38) for Russia, in (1.02-1.28) for India and in (1.08-1.82) and (1.03-1.12) for South Africa. Overall, for Brazil, India and South Africa the left-tail is higher than the right-tail dependence. The reverse is observed for Russia, whilst the upper-tail dependence for China is found to be significant only during the period 2007-2011.

5. CONCLUSIONS

Our work extends the recent literature on global portfolio hedging and diversification effects of gold-based strategies, in particular putting emphasis on the heterogeneous BRICS stock markets. While having a high growth rate, these economies still experience a high degree of vulnerability to external shocks especially to commodity dependence. We specifically probe into the nature and directionality of gold-stock market linkages by investigating not only the dynamics of the time series interdependence, but also their interactions under a time-frequency framework. Relying on a multi-scale wavelet approach and a time-varying copula methodology, we were able to reveal a strong time-varying dependence structure between gold and each of the BRICS' markets. The phase/coherence analysis shows that gold leads significantly the BRICS markets during the global financial crisis. The heterogeneity is evidenced also by the asymmetric effects derived from the GJR-GARCH volatility modeling, which exhibits highly statistically significant parameters for both markets. The lower tail is higher than the upper-tail dependence in all cases, therefore the BRICS and gold markets co-move much more in bear than in bull markets. The multi-resolution analysis uncovers the time-scale co-evolvement patterns between the two markets, with profound regions of concentrated extreme variations. Our results reveal the potential implications of equity portfolio risk diversification and hedging strategies between BRICS and commodity markets.

REFERENCES

Aguiar-Conraria, L., and Soares, M. J. 2014. The continuous wavelet transform: moving beyond uni- and bivariate analysis. *Journal of Economic Surveys* 28(2), 344-375.

Aguiar-Conraria, L., Azevedo, N., and Soares, M. J. 2008.Using wavelets to decompose the time–frequency effects of monetary policy. *Physica A: Statistical mechanics and its Applications* 387(12), 2863-2878.

Assenmacher-Wesche, K. and Gerlach, S. 2007. Money at low frequencies. *Journal of the European Economic Association* 5(2-3), 534-542.

Assenmacher-Wesche, K., Gerlach, S., and Sekine, T. 2008. Monetary factors and inflation in Japan. *Journal of the Japanese and International Economies* 22, 343–363.

Baur, D. G. (2013). The autumn effect of gold. *Research in International Business and Finance* 27(1), 1-11.

Baur, D. G., and Lucey, B. M. (2010). Is gold a hedge or a safe haven? An analysis of stocks, bonds and gold. *Financial Review* 45, 217–229.

Baur, D. G., and McDermott, T. K. (2010). Is gold a safe haven? International evidence. *Journal of Banking and Finance* 34, 1886–1898.

Bekiros, S., and Marcellino, M. (2013). The multiscale causal dynamics of foreign exchange markets. *Journal of International Money and Finance* 33, 282–305.

Breitung, J., and Candelon, B. 2006. Testing for short and long-run causality: a frequency domain approach. *Journal of Econometrics* 132, 363-378.

Conover, C. M., Jensen, G. R., Johnson, R. R., and Mercer, J. M. (2009). Can precious metals make your portfolio shine? *Journal of Investing* 18, 75–86.

Dickey, D. A., and Fuller, W. A. 1981. Likelihood ratio statistics for autoregressive time series with a unit root. *Econometrica*, 1057-1072.

Engle, R. F. 1982. Autoregressive conditional heteroscedasticity with estimates of the variance of United Kingdom inflation. *Econometrica* 50, 987–1008.

Fan, Y., and Gençay, R., 2010. Unit root tests with wavelets. *Econometric Theory* 26(5), 1305-1331

Gençay, R., B. Whitcher and F. Selçuk, 2001, Differentiating intraday seasonalities through wavelet multi-scaling. *Physica A* 289(3-4), 543–556.

Gençay, R., B. Whitcher and F. Selçuk, 2002. An *introduction to wavelets and other filtering methods in finance and economics*. Academic Press, San Diego.

Gençay, R., and Signori, D. 2015. Multi-scale tests of serial correlation. *Journal of Econometrics,* 184, 62-80.

Geweke, J. 1982. Measurement of linear dependence and feedback between multiple time series. *Journal of American Statistical Association* 77, 304-324.

Glosten, L. R., Jagannathan, R., and Runkle, D. E. 1993. On the relation between the expected value and the volatility of the nominal excess return on stocks. *The Journal of Finance* 48(5), 1779-1801.

Granger, C.W. J. 1969. Investigation causal relations by econometric models and cross-spectral methods. *Econometrica* 37, 424-38.

Gronwald, M. 2009. Reconsidering the macroeconomics of the oil price in Germany: a testing for causality in the frequency domain. *Empirical Economics* 36, 441–453.

Hammoudeh, S., Malik, F., and McAleer, M. (2011). Risk management of precious metals. *Quarterly Review of Economics and Finance* 51, 435–441.

IMF, 2015. World Economic Outlook Database. April 2015, available at http://www.imf.org/external/pubs/ft/weo/2015/01/weodata/index.aspx

Joe, H., 1997. Multivariate models and dependence concepts. *Monographs in Statistics and Probability 73. Chapman and Hall, London*

Joy, M. (2011). Gold and the US dollar: Hedge or haven?. *Finance Research Letters* 8(3), 20-131.

Lemmens, A., Croux, C., and Dekimpe, M. G. (2008). Measuring and testing Granger-causality over the spectrum: an application to European production expectation surveys. *International Journal of Forecasting* 24, 414-431.

Patton, A. J. (2006). Modelling asymmetric exchange rate dependence. *International Economic Review* 47(2), 527-556.

Ramsey, J. B., D. Usikov and G. M. Zaslavsky, 1995. An analysis of U.S. stock price behavior using wavelets. *Fractals* 3(2), 377–389.

Ramsey, J.B. and C. Lampart, 1998a. The decomposition of economic relationships by time scale using wavelets: Money and income. *Macroeconomic Dynamics* 2, 49–71.

Ramsey, J.B. and C. Lampart, 1998b. The decomposition of economic relationships by time scale using wavelets: Expenditure and income. *Studies in Nonlinear Dynamics & Econometrics* 3(1), 23-42.

Reboredo, J. C. (2013). Is gold a safe haven or a hedge for the US dollar? Implications for risk management. *Journal of Banking and Finance* 37(8), 2665-2676.

Riley, C., 2010. A new gold rush: Investing in precious metals. *Journal of Investing* 19, 95-100

Rua, A., and Nunes, L. C. 2009. International comovement of stock market returns: A wavelet analysis. *Journal of Empirical Finance* 16(4), 632-639.

Torrence, C., and Compo, G.P. 1998. A practical guide to wavelet analysis. *Bulletin of the American Meteorological Society* 79, 605–618.

Torrence, C., and Webster, P. 1999. Interdecadal changes in the ESNOM on soon system. Journal of Climate 12, 2679–2690.

TABLE 1: DESCRIPTIVE STATISTICS

	Gold	Brazil	Russia	India	China	S. Africa
Mean(%)	0.039	0.027	0.023	0.030	0.025	0.028
Std. Dev.	0.012	0.022	0.026	0.018	0.019	0.018
Skewness	-0.279	-0.248	-0.522	-0.136	-0.003	-0.333
Kurtosis	8.854	10.208	14.338	10.271	8.598	7.748
J-B	5478.87^{+}	8270.66^{+}	20543.78^{+}	8389.24^{+}	4965.59^{+}	3641.95^{+}
Q(12)	27.95^{+}	55.89^{+}	49.78^{+}	71.14^{+}	31.23^{+}	41.61^{+}
Q^2(12)	315.96^{+}	3771.09^{+}	1846^{+}	790.62^{+}	2333.04^{+}	2488.19^{+}
ARCH(12)	14.98^{+}	145.09^{+}	68.94^{+}	31.15^{+}	81.47^{+}	83.28^{+}
Correlation. vs. Gold	1	0.15	0.12	0.11	0.09	0.28
Obs.	3803	3803	3803	3803	3803	3803

Notes: J-B, Q(12), Q^2 (12) and ARCH(12) correspond to the Jarque-Bera, Ljung-Box for 12-order serial autocorrelation in raw and squared residuals, and Engle (1982) test for conditional heteroscedasticity. $^{+}$ and $^{++}$ indicate the rejection of the null at the 1% and 5% significance level, respectively.

TABLE 2: GJR-GARCH PARAMETER ESTIMATION & DIAGNOSTICS

	Brazil	Russia	India	China	S. Africa	Gold
Panel A: Estimation results of GARCH						
Parameter Estimates-mean equations						
Const(m)(%)	0.0004^{+++} (0.0003)	0.0010^{+} (0.0002)	0.0008^{+} (0.0002)	0.0005^{++} (0.0002)	0.055^{++} (0.0002)	0.0006^{+} (0.0001)
AR(1)	0.082^{+} (0.015)	0.050^{+} (0.016)	0.085^{+} (0.016)	0.052 (0.015)	0.036^{++} (0.016)	-0.044^{+} (0.014)
Parameter estimates-GARCH process						
Const(v)(10^{-4})	0.082^{+} (0.029)	0.082^{+} (0.021)	0.087^{+} (0.017)	0.032^{+} (0.009)	0.071^{+} (0.016)	0.009^{+} (0.003)
ARCH	0.009 (0.007)	0.064^{+} (0.012)	0.041^{+} (0.010)	0.024^{+} (0.006)	0.015^{+++} (0.008)	0.057^{+} (0.010)
GARCH (β)	0.918^{+} (0.018)	0.888^{+} (0.012)	0.852^{+} (0.017)	0.924^{+} (0.009)	0.901^{+} (0.013)	0.954^{+} (0.006)
GJR(γ)	0.100^{+} (0.020)	0.070^{+} (0.018)	0.148^{+} (0.027)	0.080^{+} (0.017)	0.111^{+} (0.019)	-0.027^{+} (0.011)
Student-df	9.255^{+} (1.293)	5.517^{+} (0.502)	7.168^{+} (0.842)	7.014^{+} (0.802)	11.859^{+} (1.969)	4.171^{+} (0.328)
Log (L)	9737.00	9455.70	10629.45	10460.66	10426.7	12025.95
Panel B: Diagnostic tests						
Skewness	-0.249^{+}	-0.392^{+}	-0.057^{+}	-0.087^{+}	-0.208^{+}	-0.105^{+}
Kurtosis	1.105^{+}	2.956^{+}	2.378^{+}	1.034^{+}	0.610^{+}	6.577^{+}
AIC	-5.118	-4.969	-5.593	-5.497	-5.479	-6.320
SIC	-5.106	-4.957	-5.582	-5.486	-5.468	-6.309
Q(20)	20.31[0.37]	16.05[0.65]	29.42[0.06]	32.36[0.03]	23.77[0.20]	17.29[0.56]
Q^2 (20)	15.85[0.66]	12.31[0.57]	33.14[0.02]	13.99[0.72]	28.46[0.06]	8.56[0.96]
ARCH(10)	0.93[0.51]	0.66[0.76]	1.34[0.20]	0.49[0.89]	0.52[0.87]	0.59[0.82]
J-B	202.55[0.00]	1482.70[0.00]	897.31[0.00]	177.44[0.00]	86.62[0.00]	6863.60[0.00]

Notes: +, ++ and +++ indicate the rejection of the null at the 1%. 5% and 10% levels, respectively. *Const(m)* and *Const(v)* refer to the constant terms in the mean and variance equations. JB stands for the Jarque-Bera test, Q(20) and Q^2(20) for the Ljung-Box test for autocorrelation with 20 lags. ARCH represents the Engle (1982) test for conditional heteroscedasticity. Standard errors are reported in parentheses.

TABLE 3: CONSTANT AND TIME-VARYING COPULA ESTIMATION RESULTS

Panel A: Time-invariant Copulas

	Brazil	**Russia**	**India**	**China**	**South Africa**
			Normal copula		
ρ	0.148	0.133	0.113	0.097	0.265
LogLik.	-42.497	-34.284	-24.640	-18.252	-138.603
AIC	86.99	70.56	51.28	38.50	279.20
			Clayton copula		
ρ	0.199^{+}	0.185^{+}	0.155^{+}	0.132^{+}	0.370^{+}
	(0.021)	(0.021)	(0.020)	(0.020)	(0.024)
LogLik.	56.877	50.069	36.776	27.215	158.546
AIC	-111.73	-98.13	-71.55	-52.42	-315.09
			Rotated Clayton copula		
ρ	0.154^{+}	0.129^{+}	0.108^{+}	0.084^{+}	0.293^{+}
	(0.021)	(0.020)	(0.020)	(0.019)	(0.023)
LogLik.	33.286	24.358	17.829	11.092	100.099
AIC	-64.57	-46.716	-33.65	-20.18	-198.19
			Plackett copula		
π	1.644^{+}	1.541^{+}	1.427^{+}	1.358^{+}	2.351^{+}
	(0.084)	(0.080)	(0.072)	(0.068)	(0.114)
LogLik.	45.304	34.304	23.695	18.316	138.501
AIC	-88.608	-66.60	-45.38	-34.63	-275.00
			Frank copula		
λ	0.915^{+}	0.795^{+}	0.662	0.585^{+}	1.717^{+}
	(0.100)	(0.101)	(1.001)	(0.099)	(0.199)
LogLik.	41.179	31.181	21.917	17.426	37.14
AIC	-80.357	-60.36	-41.83	-32.85	-72.28
			Gumbel copula		
δ	1.102^{+}	1.100^{+}	1.100^{+}	1.100^{+}	1.191^{+}
	(0.012)	(0.019)	(0.019)	(0.019)	(0.014)
LogLik.	51.829	39.598	27.041	11.236	141.822
AIC	-101.65	-77.19	-52.08	-20.47	-281.64
			Rotated Gumbel copula		
δ	1.114^{+}	1.105^{+}	1.100^{+}	1.100^{+}	1.212^{+}
	(0.012)	(0.011)	(0.019)	(0.019)	(0.014)
LogLik.	70.897	60.039	43.410	29.928	184.126
AIC	-139.79	-118.07	-84.81	-57.85	-366.25
			Student-t copula		
r	0.152^{+}	0.135^{+}	0.113^{+}	0.100^{+}	0.266^{+}
	(0.018)	(0.018)	(0.017)	(0.016)	(0.017)
υ	4.984^{+}	0.548^{+}	6.159^{+}	8.723^{+}	4.613^{+}
	(0.504)	(0.599)	(0.766)	(1.439)	(0.428)
LogLik.	106.694	87.556	66.800	41.222	217.664
AIC	-209.38	-171.11	-129.59	-78.44	-431.32
			Symmetrised Joe-Clayton (SJC) copula		
λ_U	0.013	0.002	0.001	0.000	0.069^{+}
	(0.013)	(0.005)	(0.002)	(0.000)	(0.019)
λ_L	0.072^{+}	0.073^{+}	0.054^{+}	0.041^{++}	0.176^{+}
	(0.021)	(0.019)	(0.018)	(0.018)	(0.019)
LogLik.	69.477	58.157	42.756	30.770	190.895
AIC	-134.95	-112.31	-81.50	-57.53	-377.78

Panel B: Time varying Copulas

	Brazil	**Russia**	**India**	**China**	**South Africa**
			Time-varying Normal copula		
Ψ_0	0.001	0.001	0.009^{++}	0.197	0.018
	(0.001)	(0.001)	(0.004)	(0.283)	(0.019)
Ψ_1	0.020^{+}	0.018^{+}	0.032^{+}	0.001	0.032^{++}
	(0.004)	(0.004)	(0.010)	(0.967)	(0.013)
Ψ_2	2.002^{+}	2.001^{+}	1.903^{+}	0.0002	1.951^{+}
	(0.006)	(0.006)	(0.044)	(0.995)	(0.086)
LogLik.	67.096	58.991	39.165	18.252	149.677
AIC	-128.18	-111.97	-72.32	-30.49	-293.34
			Time-varying rotated Gumbel Copula		
Ψ_0	1.324^{++}	0.466^{++}	-0.634^{+}	2.225^{+}	-0.140
	(0.527)	(0.745)	(0.237)	(0.101)	(0.105)
Ψ_1	-0.352	0.171	0.951^{+}	-1.852^{+}	0.621^{+}
	(0.402)	(0.548)	(0.175)	(0.122)	(0.057)
Ψ_2	-1.893^{+}	-1.033^{++}	-0.320^{+++}	0.098^{++}	-0.536^{+}
	(0.264)	(0.444)	(0.157)	(0.049)	(0.131)
LogLik.	96.014	80.375	52.475	33.816	221.293
AIC	-186.02	-154.74	-98.944	-61.62	-436.58
			Time-varying SJC copula		
Ψ_0	1.654	3.241^{++}	-1.031	-13.681^{+}	1.719
	(1.308)	(1.582)	(3.166)	(1.000)	(1.238)
Ψ_1	-16.774^{+}	-25.000^{+}	-14.404	-0.001	-15.384^{+}
	(4.860)	(6.627)	(12.328)	(1.000)	(4.300)
Ψ_2	-5.045	-5.037^{+++}	-0.003	-0.000	-1.167
	(4.452)	(2.750)	(1.004)	(1.000)	(2.310)
Ψ_3	0.527	1.547^{+++}	1.488	-3.384^{+}	-1.399^{+}
	(1.549)	(0.944)	(1.382)	(0.600)	(0.331)
Ψ_4	-10.917^{++}	-13.099^{+}	-14.333^{+}	-0.057	-2.754^{+}
	(5.207)	(2.936)	(5.289)	(1.000)	(0.963)
Ψ_5	1.086	-3.941	-2.524	-0.020	3.604^{+}
	(2.454)	(2.591)	(2.719)	(0.999)	(0.468)
LogLik.	93.101	78.264	49.803	30.076	228.886
AIC	-174.17	-144.50	-87.58	-48.13	-445.75

Notes: The table reports the maximum likelihood estimates for the different copula models. Standard error values are presented in parentheses and Akaike information criterion (AIC) values adjusted for small-sample bias are provided for the different copula models. The minimum AIC value (in bold) indicates the best copula fit.
+, ++ and +++ indicate significance at the 1%. 5% and 10% level respectively.

FIGURE 1: BRICS AND GOLD LOG-PRICE LEVELS

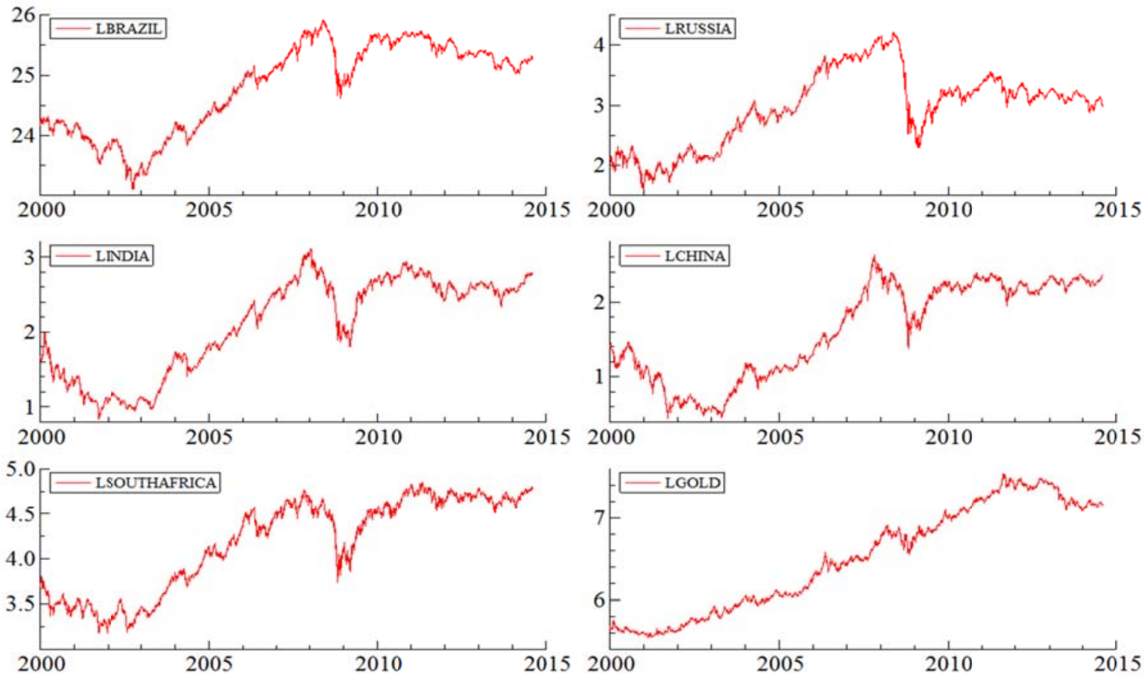

Notes: The data span the period 03 January2000 - 31 July 2014 (Datastream International)

FIGURE 2: BRICS AND GOLD LOG-RETURNS

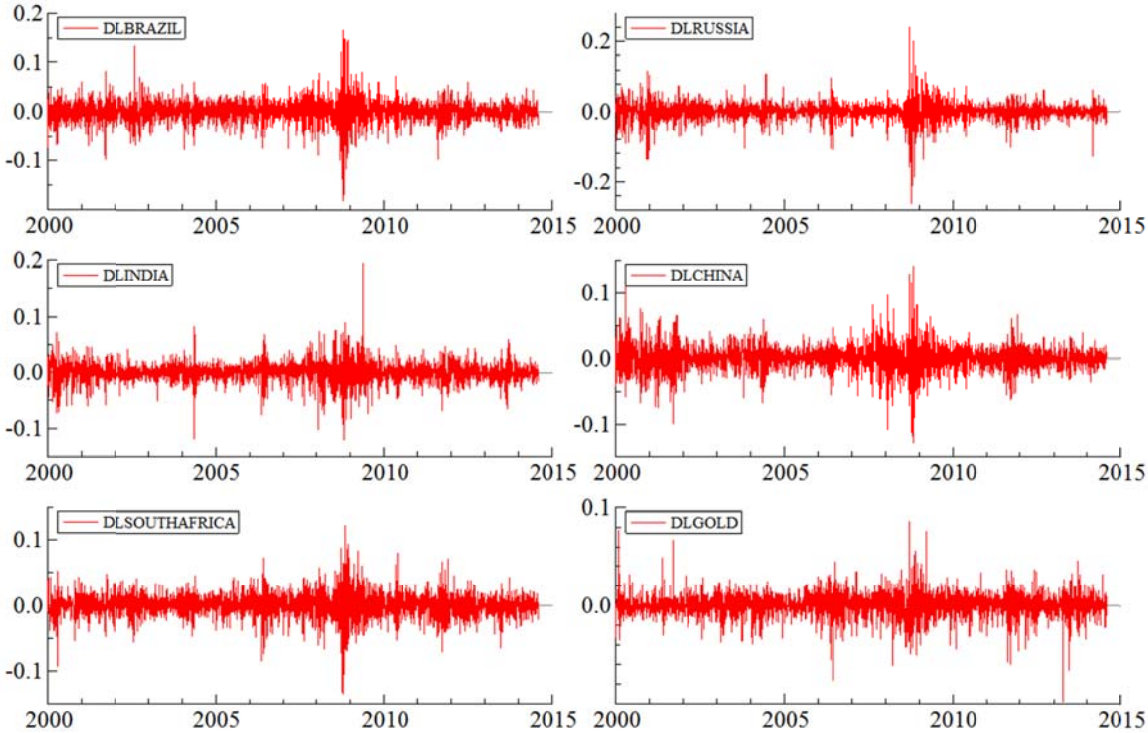

Notes: The data span the period 03 January2000 - 31 July 2014 (Datastream International)

FIGURE 3: CROSS-WAVELET COHERENCE BETWEEN THE BRICS AND GOLD MARKETS

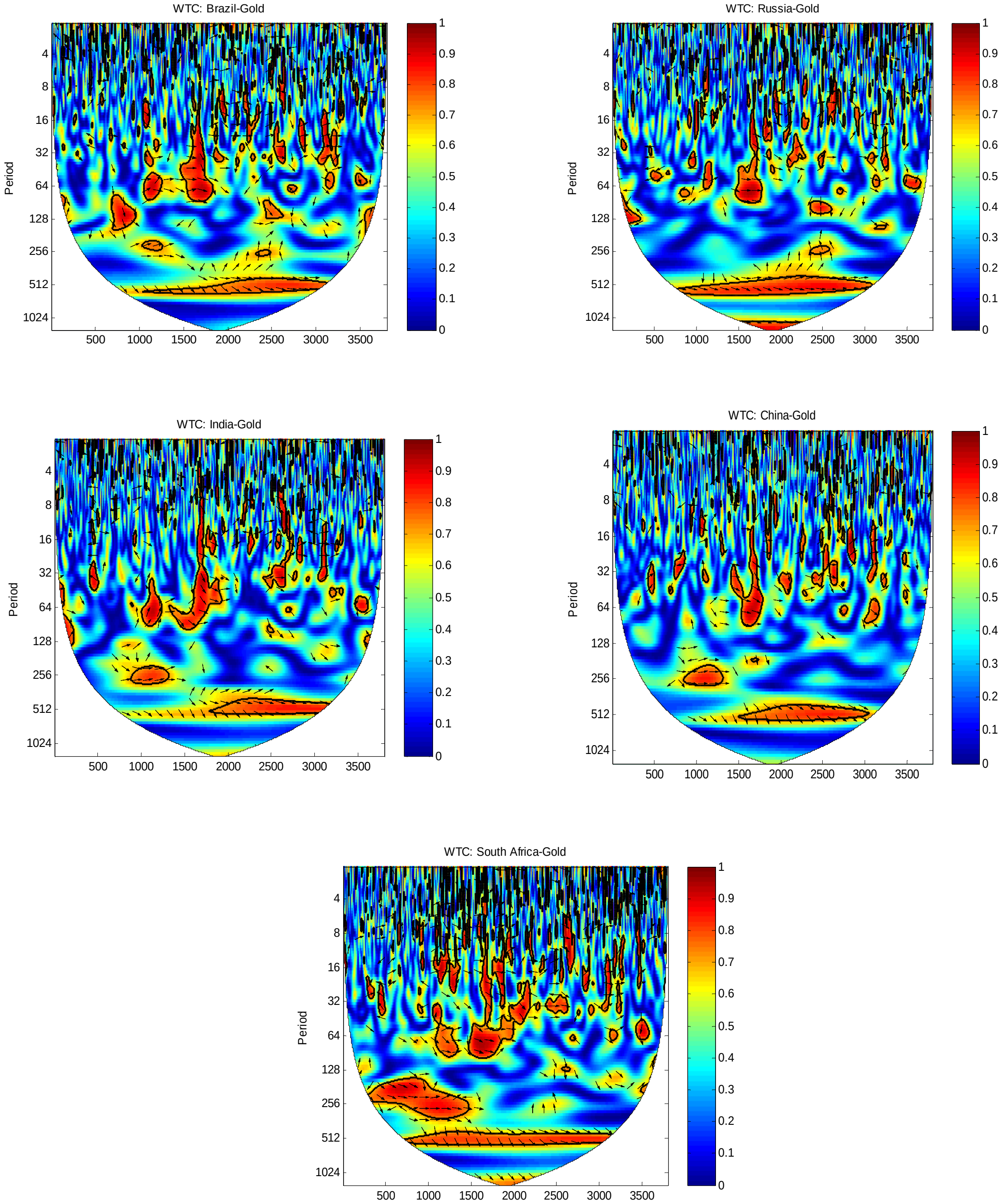

Notes: Phase arrows indicate the direction of co-movement among the returns series of the BRICS' equity markets and Gold pairwise. Arrows pointing to the right signify perfectly phased variables. The direction "right-up" indicates lagging gold market, whilst the "right-down" direction indicates leading gold vs. the BRICS. Arrows pointing to the left signify out-of-phase variables. The direction "left-up" indicates leading Gold, whilst the "left-down" direction indicates a lagging Gold market. In-phase variables represent a cyclical relationship and out-of-phase (or anti-phase) variables show anti-cyclical behavior. The thick black contour lines indicate the 5% significance intervals estimated from Monte Carlo simulations with phase-randomized surrogate series. The cone of influence, which marks the region affected by edge effects, is shown with a lighter shade black line. The color legend for spectrum power ranges from Blue (low power) to Red (high power). Y-axis measures frequency (scale) and X-axis represents the time period studied ranging from 500, 1000, 1500, 2000, 2500, 3000 to 3500 obs. The corresponding dates are 2001$M_{12}D_{03}$, 2003$M_{11}D_{03}$, 2005$M_{10}D_{03}$, 2007$M_{09}D_{03}$, 2009$M_{08}D_{03}$, 2011$M_{07}D_{04}$, and 2013$M_{06}D_{03}$ respectively. The starting and ending dates are 2000$M_{01}D_{04}$ and 2014$M_{07}D_{31}$, respectively.

FIGURE 4: FREQUENCY-DOMAIN CAUSALITY BETWEEN THE BRICS AND GOLD MARKETS

Brazil-Gold

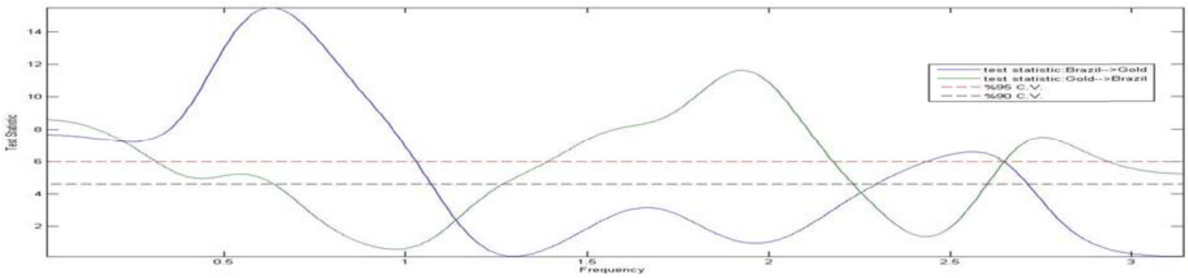

Russia-Gold

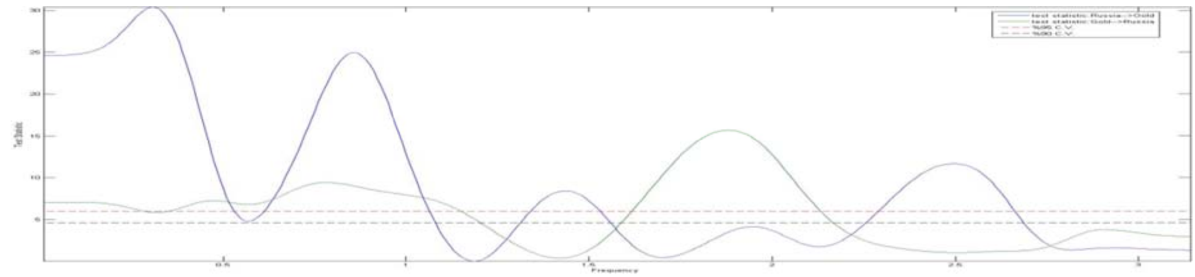

India-Gold

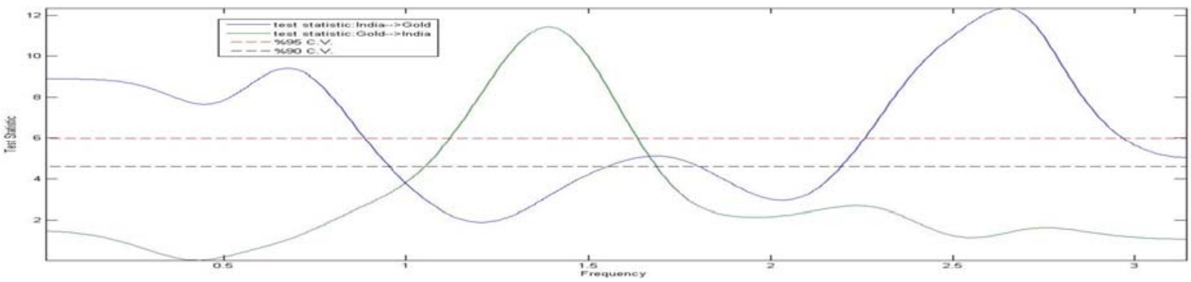

China-Gold

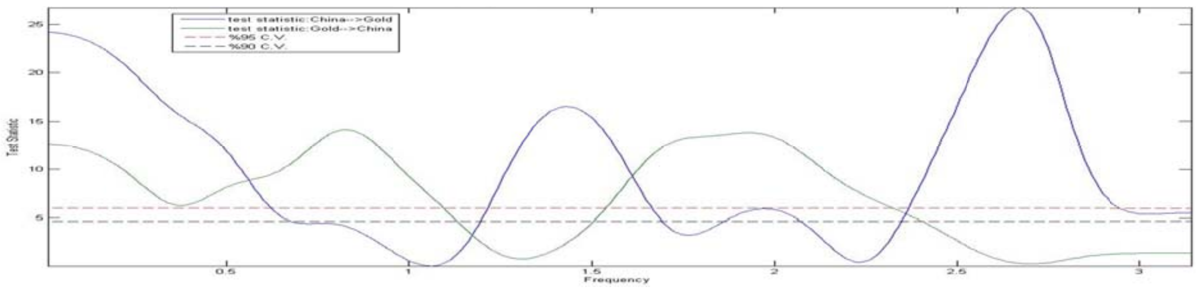

South Africa-Gold

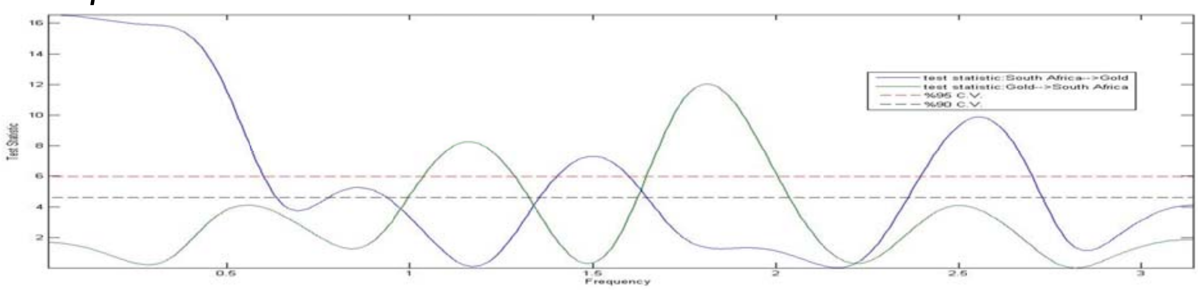

Notes: The frequency ϑ on the horizontal axis can be translated into a cycle (or periodicity) of T months as denoted in the formula $T = 2\pi / \vartheta$. Four bands or time horizons are considered: very short horizons with (0, 0.5), short-run horizons (0.5, 1.5), medium-run with (1.5, 2.5) and longest periods with a range of (2.5, π). The short-term fluctuations are presented at the right-end whilst the long-run frequencies at the left end. Dotted lines denote the 5% and 10% levels of significance. The test statistics are presented in the vertical axis.

FIGURE 5: TVP-NORMAL COPULA DEPENDENCE MEASUREMENT

Brazil

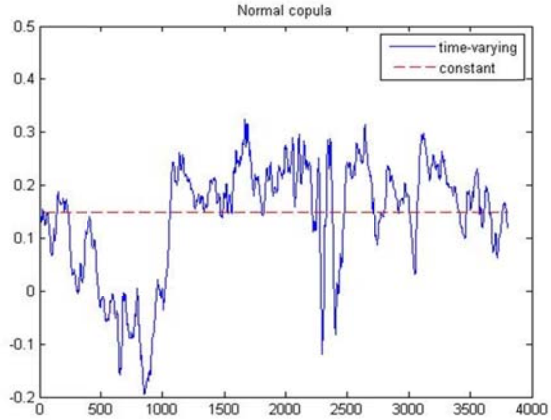

Russia

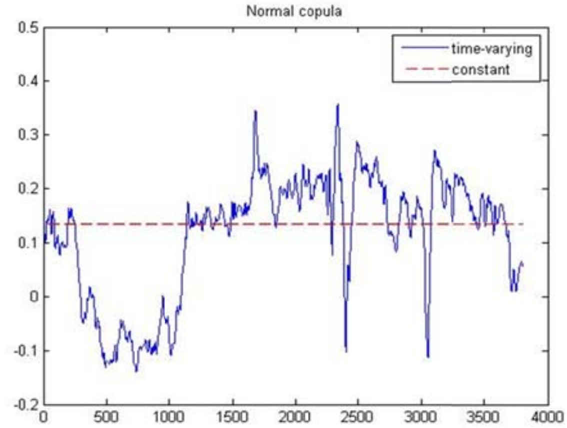

India

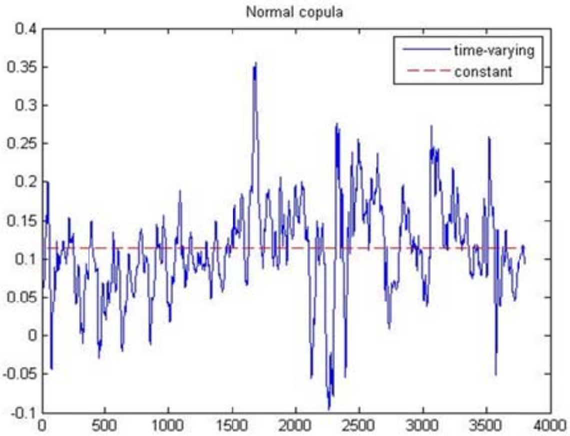

China

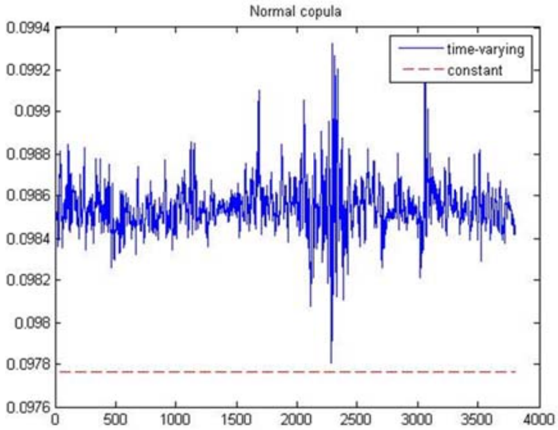

South Africa

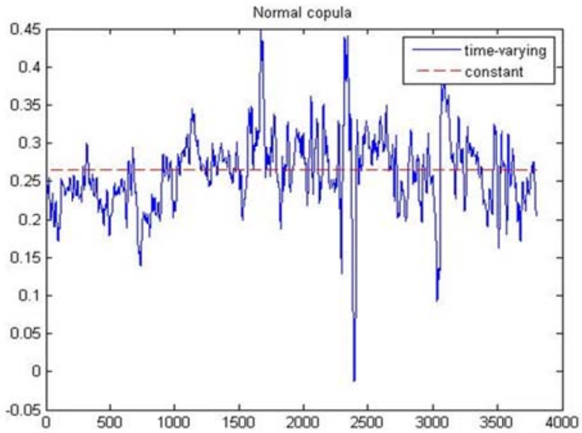

Notes: In the *X*-axis the time period is divided into 500, 1000, 1500, 2000, 2500, 3000 to 3500 daily obs. corresponding to the following dates: $2001M_{12}D_{03}$, $2003M_{11}D_{03}$, $2005M_{10}D_{03}$, $2007M_{09}D_{03}$, $2009M_{08}D_{03}$, $2011M_{07}D_{04}$, and $2013M_{06}D_{03}$. The starting and ending dates are $2000M_{01}D_{04}$ and $2014M_{07}D_{31}$, respectively.

FIGURE 6: TVP-ROTATED GUMBEL COPULA DEPENDENCE MEASUREMENT

Brazil

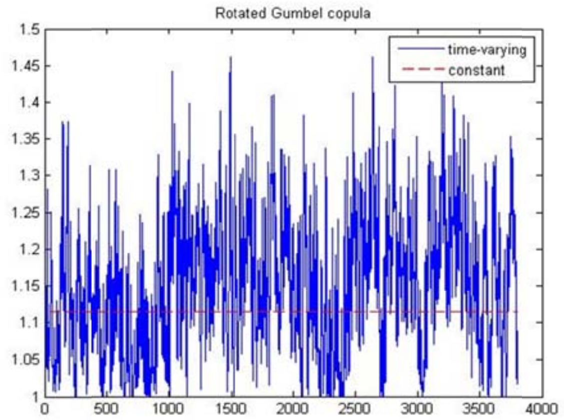

Russia

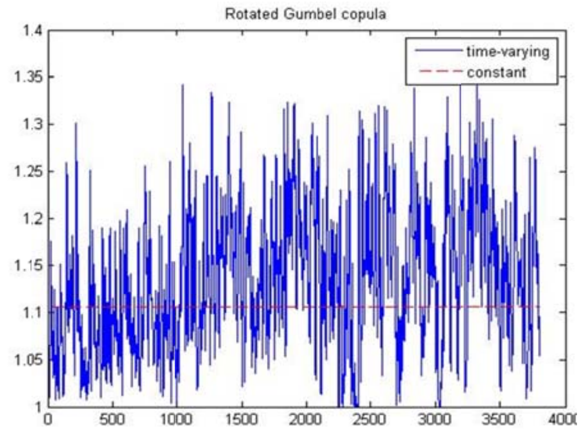

India

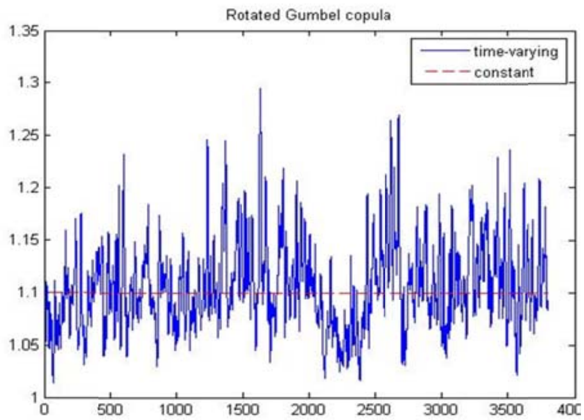

China

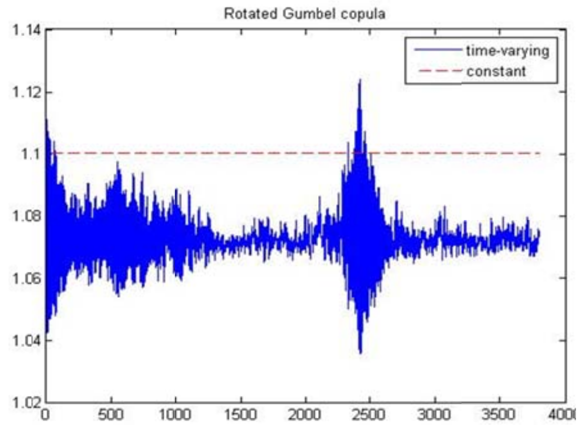

South Africa

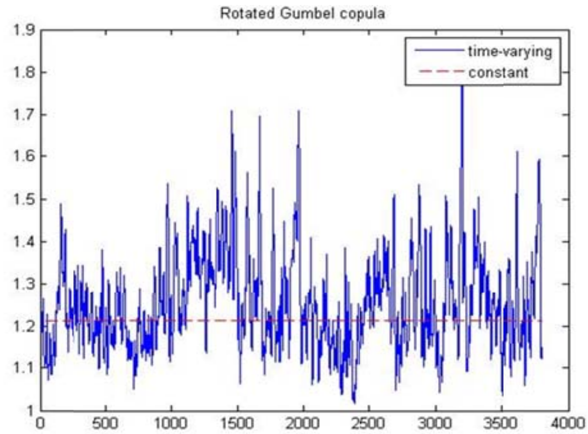

Notes: In the *X*-axis the time period is divided into 500, 1000, 1500, 2000, 2500, 3000 to 3500 daily obs. corresponding to the following dates: 2001M$_{12}$D$_{03}$, 2003M$_{11}$D$_{03}$, 2005M$_{10}$D$_{03}$, 2007M$_{09}$D$_{03}$, 2009M$_{08}$D$_{03}$, 2011M$_{07}$D$_{04}$, and 2013M$_{06}$D$_{03}$. The starting and ending dates are 2000M$_{01}$D$_{04}$ and 2014M$_{07}$D$_{31}$, respectively.

FIGURE 7: TVP-SJC COPULA DEPENDENCE MEASUREMENT

Brazil

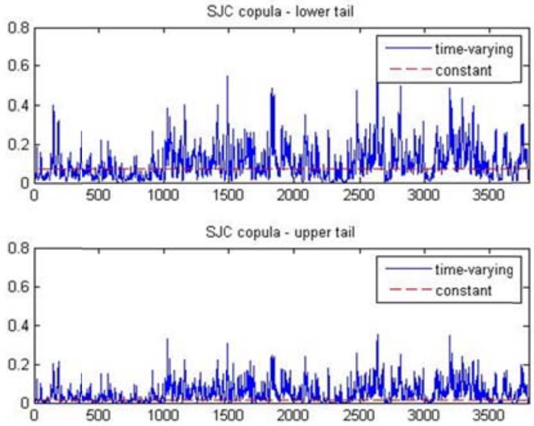

Russia

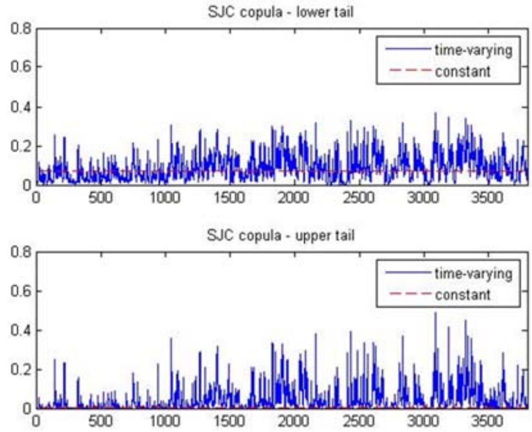

India

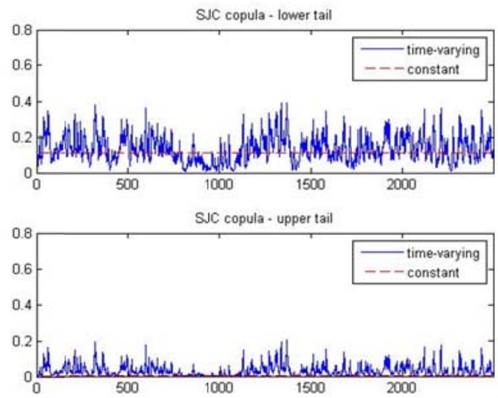

China

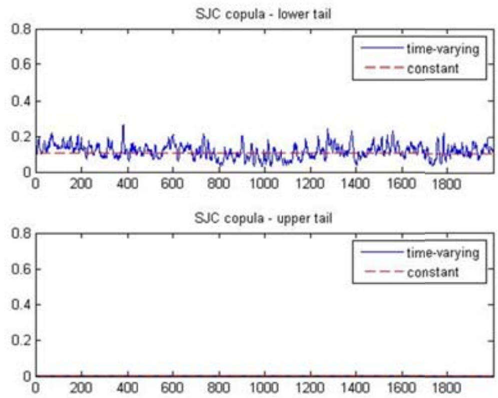

South Africa

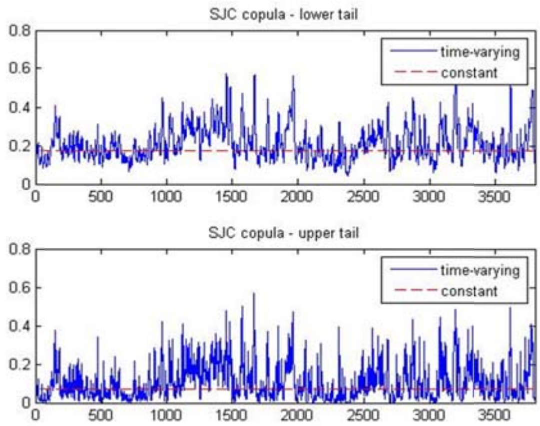

Notes: In the *X*-axis the time period is divided into 500, 1000, 1500, 2000, 2500, 3000 to 3500 daily obs. corresponding to the following dates: 2001$M_{12}D_{03}$, 2003$M_{11}D_{03}$, 2005$M_{10}D_{03}$, 2007$M_{09}D_{03}$, 2009$M_{08}D_{03}$, 2011$M_{07}D_{04}$, and 2013$M_{06}D_{03}$. The starting and ending dates are 2000$M_{01}D_{04}$ and 2014$M_{07}D_{31}$, respectively for Brazil, Russia and South Africa. For the TVP-SJC in particular the time sample estimation for India is 2005M_{01} and 2014M_{12} whilst for China 2007M_{01} to 2011M_{12} respectively.